On the Experimental Estimation of Surface Enhanced Raman Scattering (SERS) Cross Sections by Vibrational Pumping

R. C. Maher* and L. F. Cohen

The Blackett Laboratory, Imperial College London, Prince Consort Road, London SW7 2BW, United Kingdom

E. C. Le Ru and P. G. Etchegoin

The MacDiarmid Institute for Advanced Materials and Nanotechnology, School of Chemical and Physical Sciences, Victoria University of Wellington, PO Box 600 Wellington, New Zealand

Received: May 1, 2006; In Final Form: July 18, 2006

We present an in-depth analysis of the experimental estimation of cross-sections in surface enhanced raman scattering (SERS) by vibrational pumping. The paper highlights the advantages and disadvantages of the technique, pinpoints the main aspects and limitations, and provides the underlying physical concepts to interpret the experimental results. Examples for several commonly used SERS probes are given, and a discussion on future possible developments is also presented. Obtaining good estimates of SERS cross-sections is, in general, an extremely hard problem and has been a longstanding ambition of the SERS community for reasons that go from the purely applied (quantification of signals) to the more fundamental (comparisons of theoretical electromagnetic enhancement factors with experiment). Any method that can produce a standard protocol for the estimation of cross-sections is, accordingly, of great interest and an effort to understand its principles and limitations is required.

Introduction

In the past decade, surface enhanced raman scattering (SERS)[1] has made rapid progress toward applications. With a sensitivity rivaling fluorescence in some cases, and a much higher structural specificity, SERS is a highly attractive technique, being developed simultaneously within the field of plasmonics. Progress toward different uses of SERS in practical applications has been steady. New substrates including arrays of inverted pyramids,[2] silver pillar and toroid arrays,[3] adaptive silver films,[4] and metallic nano-shells[5] have been demonstrated. In addition, many molecules relevant to a myriad of applications such as glucose,[6] proteins,[7] DNA,[8] a wide range of medicinal drugs,[9−11] and substances for forensic science[12] have been characterized. On the other hand, the understanding of some fundamental aspects of the phenomenon is still incomplete and, in some cases, controversial. Although a full understanding is sometimes not essential for the development of applications, there can be no denying in the fact that a better comprehension is desirable.

Optical pumping of vibrational modes was first suggested in 1996 based primarily on the observed dependence of the anti-Stokes/Stokes (aS/S) ratio with incident laser power,[13] and it was suggested that this could be a possible tool to estimate SERS cross-sections. However, the interpretation of these experimental results has been the subject of considerable debate in the literature, with many authors simply denying the existence of pumping and attributing the experimental observations to either laser-heating, resonance effects, or combinations thereof.[14−17] Over a series of previous papers we have suggested the investigation of the aS/S-ratio as a function of temperature (T) as an alternative method for the observation of pumping.[18−20] In a recent paper, we provided definitive evidence for the existence of vibrational pumping under SERS conditions thereby bringing to conclusion one aspect of this complex problem.[20] Here, we address another aspect, namely the problems associated with estimating the SERS cross-section using this method, and we extend our analysis to include different analytes and laser excitations. We also highlight several outstanding issues which were not considered previously.[20]

Before we go into the details, we briefly review the necessary concepts for understanding aS/S-ratios and vibrational pumping in SERS. The method we are going to present has not been widely used, and therefore, we review the historical background and also its peculiarities and limitations. The discussion has some natural overlap with our previous papers,[18−20] but it is presented here for the sake of completeness, the convenience of the reader, and future reference for forthcoming work in progress. This will inevitably result in a somewhat lengthy introductory section where the principles of the method are laid down. The next sections are fully devoted to this and are followed by a section at the end with a practical experimental demonstration of SERS cross-section determination for several standard probes.

II. A Brief Description of SERS Pumping

A. The Anti-Stokes/Stokes Ratio. Let us consider the different contributions to the population of a single vibrational level at temperature T during a SERS measurement; we can identify two main contributions: (*i*) the laser itself which pumps vibrations through Stokes Raman processes with a rate proportional to its intensity (I_L) and to the Raman−Stokes cross-section (σ_S), and (*ii*) thermal excitation populating the level. Vibrations remain in the level with a finite lifetime τ, which encompasses

* Corresponding author phone: 44 (0)20 7594 7587; fax: 44 (0)20 7594 7580; E-mail: Robert.Maher@imperial.ac.uk.

10.1021/jp0626521 CCC: $33.50
Published on Web 09/09/2006

all possible relaxation mechanisms, such as intramolecular vibrational relaxation IVR (anharmonic processes) or external relaxation mechanisms. There are other possible secondary mechanisms, such as relaxation through anti-Stokes Raman processes, or excitation to higher vibrational levels. It is possible to write rate equations for the detailed dynamics of vibration populations in such a system.[16] In the regime of weak pumping (which is the only case considered here), where the vibrational population remains small, $n \ll 1$, it is sufficient to consider only the two main mechanisms, and the rate equation for n can then be written as follows:

$$\frac{dn}{dt} = \frac{\sigma_S I_L}{\hbar\omega_L} + \frac{\exp(-\hbar\omega_\nu/k_B T)}{\tau} - \frac{n}{\tau} \quad (1)$$

where σ_S is the Raman−Stokes cross-section, I_L the intensity (power per surface area) of the laser, $\hbar\omega_L$ the energy of an exciting photon ($n_L = I_L/\hbar\omega_L$ is the number of incident photon per unit time and surface area), and $\hbar\omega_\nu$ the energy of the vibration. The first term on the right is the number of vibrations per unit time being pumped into the level by the action of the laser, while the second and third terms are the contributions of thermal excitation and population relaxation, respectively. In the steady state $dn/dt = 0$. Generally, σ_S is very small, so when I_L is small, the pumping contribution is negligible, and the vibrational population is dominated by thermal effects; i.e., $n = \exp(-\hbar\omega_\nu/k_B T)$ is given by a Boltzmann factor. When I_L or σ_S is increased (so that there is a significant pumping contribution to the population of the level) n becomes the following:

$$n = \frac{\tau\sigma_S I_L}{\hbar\omega_L} + e^{-\hbar\omega_\nu/k_B T} \quad (2)$$

where the pumping term is clearly distinguished from the thermal contribution.

In addition, for an ensemble of N molecules, the Stokes−Raman signal is given by $I_S = N\sigma_S I_L$, while the anti-Stokes signal is given by $I_{aS} = nN\sigma_{aS} I_L$, leading to the following:

$$I_{aS} = \left(\frac{\tau\sigma_S I_L}{\hbar\omega_L} + e^{-\hbar\omega_\nu/k_B T}\right) N\sigma_{aS} I_L \quad (3)$$

Moreover, taking the ratio of the anti-Stokes to the Stokes intensities (ρ), we have the following:

$$\rho = \frac{I_{aS}}{I_S} = \frac{\sigma_{aS}}{\sigma_S} n = An \quad (4)$$

where A is the *asymmetry factor* (extensively discussed in refs 18−20). A includes not only any possible difference between anti-Stokes and Stokes cross sections arising from resonance effects (due either to plasmon resonances or to resonant Raman scattering for a resonant analyte), but also the standard wavelength dependence of Raman processes $A_{\omega\nu} = (\omega_L + \omega_\nu)^4/(\omega_L - \omega_\nu)$.[4] ρ can be expressed as follows:

$$\rho = A\left[\frac{\tau\sigma_S I_L}{\hbar\omega_L} + e^{-\hbar\omega_\nu/k_B T}\right] \quad (5)$$

This simple model shows that the Stokes−Raman signal always remains linearly dependent on I_L. The anti-Stokes signal also shows a linear dependence with power when pumping is negligible. But when pumping dominates over thermal effects, then I_{aS} varies quadratically with power while the aS/S-ratio is linearly dependent on I_L.

The original work by Kneipp et al.[13] used rhodamine 6G (RH6G) and crystal violet (CV) (two commonly used SERS active dyes) under 830 nm excitation at room temperature (RT). The argument for pumping was primarily based on two observations: (i) the aS/S-ratios were shown to be larger than expected for a Boltzmann factor, and (ii) the *power dependence* of the signal at RT (where the thermal contribution is likely to dominate, or be important) was quadratic. This observation of a nonlinear dependence of the anti-Stokes intensities with power (resulting in a linear dependence in the aS/S-ratio) was thought to provide strong evidence for vibrational pumping in SERS. Further measurements on carbon nanotubes[17] and a DNA-base[21] supported these initial results. The arguments against this original interpretation are summarized in the following subsection.

B. Resonance and Heating Effects. Haslett et al.[15] were the first to seriously question the existence of vibrational pumping as revealed in the original studies. Extensive measurements were made under similar conditions with a number of both resonant and nonresonant molecules. They observed an anomalous ratio for all the resonant molecules tested which was independent of power until photobleaching occurred. No anomaly was observed in the case of the nonresonant molecules. It was concluded that the anomalous ratios observed in the original papers were the result of "hidden" resonances rather than pumping.[22] Brolo et al.[14] also concluded that the observed anomalous ratio could be explained by resonances. These resonances are accounted for by the asymmetry factor A in the model of the previous section. In the absence of pumping, the aS/S-ratio is predicted to be

$$\rho = A\exp\left(-\frac{\hbar\omega_\nu}{k_B T}\right). \quad (6)$$

It is clear that the A factor can indeed result in anomalous ratios (different from the Boltzmann factor), even in the absence of pumping.

Furthermore, it was suggested that the observed power dependence was not the effect of pumping but rather laser heating. The effect of heating on ρ in the absence of pumping can be simply understood by including it in eq 6. The real temperature of the probed molecule, T_h, may be different to the nominal temperature T because of heating effects, either in the SERS substrate or in the molecule itself.[16] By writing $T_h = T + \Delta T$ and assuming that $\Delta T \ll T$ we can obtain the corresponding ratio, ρ_h, by expanding eq 6 as follows:

$$\rho_h = A\exp\left(-\frac{\hbar\omega_\nu}{k_B T}\right)\exp\left(\frac{\hbar\omega_\nu}{k_B T}\frac{\Delta T}{T}\right) \quad (7)$$

This expression first shows that heating can also result in an anomalous aS/S ratio, even when $A \approx 1$. Moreover, it can have an important impact on the power dependence of ρ, because ΔT should increase with I_L. We can assume in a first approximation that $\Delta T \approx \alpha I_L$. The above expression shows that laser heating should then result in an exponential increase of ρ_h with I_L. However, in many cases of interest, the argument in the second exponential is small compared to 1, and eq 7 can then be further expanded to give the following:

$$\rho_h = A\exp\left(-\frac{\hbar\omega_\nu}{k_B T}\right)\left(1 + \frac{\hbar\omega_\nu}{k_B T}\frac{a}{T} I_L\right). \quad (8)$$

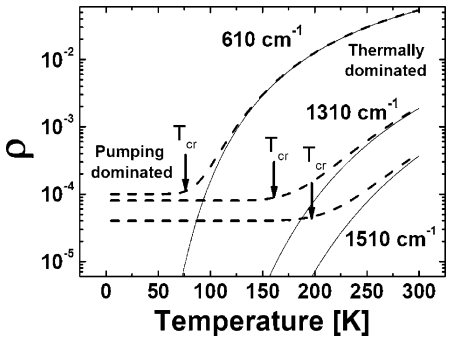

Figure 1. Schematic diagram showing the temperature dependence of the anti-Stokes/Stokes ratio (ρ) for several different Raman modes. We have assumed here $A = 1$ for simplicity and have used three characteristic Raman modes of rhodamine 6G for the example. The solid lines represent the ratio when there is no pumping contribution (Boltzmann factor). The dashed lines show the result of including pumping as given by eq 5. There are two regimes, one at high temperature where the thermal contributions dominate and the ratio is similar to what is expected if no pumping were present. The second occurs at low *T*'s where the contribution of pumping becomes significant relative to the thermal contribution. We refer to the crossover point between these two regimes as the T_{cr} (indicated by the arrows in this figure). T_{cr} generally occurs at higher *T*'s for higher energy modes due to the different influence of the exponential factor for different mode energies in eq 5. See the text for further details.

A linear dependence of ρ with I_L (or equivalently a quadratic dependence of I_{aS} with I_L) *can then equally be the result of conventional heating effects or pumping*. Such an observation is therefore insufficient to demonstrate the presence or not of vibrational pumping. We also note that heating effects can also explain the mode-dependent behavior observed in the original work,[13] as the argument of the second exponential in eq 7 depends on the mode energy $\hbar\omega_\nu$.

C. Temperature Dependence of the aS/S Ratios. Most studies have concentrated on finding evidence for SERS pumping at room temperature (RT), in particular by studying the power dependence of the aS/S ratio. It is true that the huge enhancements in SERS conditions greatly increases the contribution from pumping, but may also contribute to an increased heating (in particular directly in the probe molecules). At room temperature (RT) and above, the thermal contribution to ρ is relatively large ,and in many cases dominates, such that $\rho \approx A \exp(-\hbar\omega_\nu/k_BT)$. The study of vibrational pumping at RT therefore involves measuring small departures from an already existing (large) thermal population. Moreover, as the previous discussion has shown it is also extremely difficult to distinguish the relative contributions of pumping and heating at RT.

A more practical approach is to study the temperature dependence of the aS/S ratios, and in particular the low-temperature regime where thermal effects are expected to be completely negligible compared to any other mechanisms, and in particular pumping. The temperature dependence can be directly studied using the model presented so far. Figure 1 summarizes the different scenarios for aS/S-ratios as a function of temperature. The solid lines show the variation of the ratio with *T* when pumping is absent; i.e., an exponential decrease as *T* decreases, following the Boltzmann factor $\exp(-\hbar\omega_v/k_BT)$. The dashed lines show the case when pumping is present. At high *T*s the ratio is approximately the same as if pumping were absent. This is the *thermally dominated regime*. As *T* is decreased, there is a crossover to a *pumping-dominated regime*, where the ratio reaches a plateau. We refer to the crossover temperature between these two regimes as T_{cr}; indicated by arrows in Figure 1. The crossover occurs when pumping and thermal terms in eq 5 are comparable, which occurs for the following:

$$k_BT_{cr} \approx \hbar\omega_\nu \left[\ln\left(\frac{\hbar\omega_L}{\tau\sigma_S I_L}\right)\right]^{-1} \quad (9)$$

The crossover occurs at a larger temperature for higher powers I_L, for which pumping is stronger, but also for higher energy peaks (with a larger $\hbar\omega_\nu$), for which thermal excitation is weaker.

Below T_{cr} each mode is "locked" into an effective temperature $T_{eff} \sim T_{cr}$ as far as the populations *n* of the levels is concerned, and this temperature is different for different modes accounting for a transition to a *pumping-dominated regime* in which there is no thermal equilibrium among the populations of different levels but rather fixed populations maintained by the pumping process. This aspect has been emphasized already in ref 20. In the pumping-dominated regime, the aS/S-ratio is constant and equal to $\rho = A\tau\sigma_S I_L/(\hbar\omega_L)$. $I_L/(\hbar\omega_L)$ can be estimated to a high degree of accuracy for a given experimental setup. If $A = 1$ (no asymmetry between σ_S and σ_{aS}), we can therefore deduce the product $\tau\sigma_S$ from the plateau in the aS/S-ratio below T_{cr}. In general, and in particular under SERS conditions, $A \neq 1$, but its value can be determined from aS/S ratios at room temperature (where the effect of pumping is negligible). In practice, a fit of the experimental data over the whole temperature range with two parameters enables us to determine both *A* and $\tau\sigma_S$.[20] Nevertheless, the problem of estimating τ still needs to be circumvented to determine the SERS cross-section σ_S itself.

By reducing *T*, the contribution from pumping becomes dominant, making measurements much easier and more reliable. It also simplifies greatly their interpretation. But the main advantage is that it enables one to unambiguously rule out heating effects as an alternative explanation. As discussed, the appearance of plateaus for $T < T_{cr}$ in Figure 1 is a clear characterization of the pumping-dominated regime. Note that it does not mean that heating is absent, but simply that its effect on aS/S-ratios is negligible (relative to the pumping contribution); for as long as a plateau is observed, vibrational pumping must occur. Moreover, the value of ρ in the plateau region (from which we will infer SERS cross-sections) is independent of heating.

Studies of the temperature dependence of ρ therefore provide a more conclusive demonstration of SERS pumping. However, the technique is not without its drawbacks. To extract SERS cross-sections for the method discussed here there are several issues that need special attention as described below. These issues have been entirely overlooked in previous studies of SERS pumping.

III. Practical Estimation of Cross-Sections from Vibrational Pumping

Several issues need to be considered in the practical determination of SERS cross-sections via vibrational pumping. Not all of them can be resolved satisfactorily and we have to include some ad-hoc approximations in order to obtain estimates of the cross sections. While there is nothing intrinsically wrong with this, it is necessary to be aware of the range of validity of the estimates in order to be able to comprehend the current limitations of the method as proposed. Many of these limitations concern the absolute values of the cross sections but are not serious limitations for relative comparisons.

A. SERS Cross-Sections. The pumping process under SERS conditions has been the subject of considerable discussion in

the literature. In particular with respect to the precise meaning of the cross section σ_S that is extracted from the measurements. It is worth mentioning here that, in many situations in Raman (and particularly in SERS), we talk plainly about the cross-section, while in reality there are several possible cross-sections: (*i*) The differential radiative cross-section, $d\sigma/d\Omega$, is the closest to what is measured in a typical experiment. It has been shown[31] that in SERS conditions, it is enhanced by a factor of the order of the fourth power of the local field enhancement factor: $|E_{Loc}/E_0|^4$. (ii) The total radiative cross-section σ_{Rad} is simply the sum over all directions of the differential cross-section. In Raman scattering, neglecting depolarization effects, it is simply obtained from $\sigma_{Rad} \approx (8\pi/3)d\sigma/d\Omega$, which comes from the $\cos^2\theta$ dependence of the radiation profile. In SERS, σ_{Rad} may not show exactly the same enhancement as the differential cross-section because the radiation profile may be different under SERS conditions. The enhancement will, however, remain of the same order of magnitude, i.e., $|E_{Loc}/E_0|^4$. (iii) In SERS conditions, some Raman photons may be absorbed by the substrate and therefore not be detected in the far-field. One can, therefore, define a *total* Raman cross-section, $\sigma_{Tot} > \sigma_{Rad}$, which includes both radiated and nonradiated Raman photons. For positions of very high field enhancement (those of interest here), σ_{Tot} is close to σ_{Rad} in a first approximation (i.e., nonradiative effects are small).

The total cross-section characterizes the number of scattered Raman photons. For each of these photons, exactly one quantum of vibration is created (Stokes) or destroyed (anti-Stokes). It is, therefore, the total cross-section that governs vibrational pumping effects under SERS conditions. This could potentially be different to the differential radiative cross-section, which is what is measured in a standard SERS experiment. Two modes of the same molecule, but with different Raman tensor symmetries could, for example, show a different ratio between total and differential cross-sections. Theses differences, however, are small compared to the magnitude of the SERS enhancements and are therefore ignored in our analysis. This could lead potentially to inconsistencies among cross-sections for different modes if they have different symmetries, or if they happen at frequencies where the nonradiative contributions are different. We will not insist on this distinction in the following.

Finally, as discussed above, it has been argued[15] that the pumping effect, characterized by σ_{Tot} should only be proportional to $|E_{Loc}/E_0|^2$ instead of a power of 4. However, a power of 4 in the differential cross-sections $d\sigma/d\Omega$ is required to explain the observation of SERS from single molecules[27] and has also been justified by theoretical arguments.[31] Since σ_{Tot} is obtained by integration of $d\sigma/d\Omega$, it must be of the same order of magnitude unless the radiation profile is extremely unidirectional. There are no experimental or theoretical arguments to support such an extreme unidirectionality. For example, a model SERS hot-spot at a junction between two spheres behaves essentially like a dipole[32] and a simple $\cos^2\theta$ is predicted. The pumping cross-section σ_{Tot} should, therefore, exhibit the power of 4 enhancement and be of the same order of magnitude as cross-sections inferred from direct SERS measurements.

B. Vibrational Lifetimes. We summarize, in this subsection, the different aspects of the problem of lifetime estimation for the purpose of obtaining SERS cross-sections.

Ultimately, the observation of a crossover from a thermally dominated to a pumping-dominated aS/S-ratio leads to an estimation of both the asymmetry factor A and the product $\tau\sigma_S$. An estimation of σ_S itself requires the knowledge of τ, as pointed out before. The latter cannot be directly obtained, in general, from the SERS spectrum potentially leading to a serious limitation of this technique. In the first report of cross-section estimation via vibrational pumping[13] a lifetime of $\tau \sim 10$ ps was simply estimated without any reference to the experimental data.

To improve upon this, we need to make a series of assumptions. The validity of these assumptions needs to be evaluated on a case-by-case basis and the results obtained for the cross-section have to be interpreted within these approximations/assumptions. Let us first review the problems associated with trying to extract lifetimes from the SERS spectra.

- Raman peaks in molecules have line shapes which are seldom pure Lorentzians and have several contributions to their natural widths; a subject of a longstanding history in spectroscopy.[23] The observed line width has typically contributions from (*i*) groups of Raman modes piled up together in narrow energy regions; (*ii*) inhomogeneous broadening, (*iii*) phase coherence relaxation, and (*iv*) population relaxation. The last two are also known as the *off-diagonal* (dephasing) and *diagonal* (population) relaxation times in density matrix formalism,[23] respectively, and are part of the *homogeneous broadening* of the peak. These relaxation times are different from mode to mode and cannot be easily separated from the observed line width in a plain SERS spectrum. The population relaxation is the one we need (τ) for the estimation of σ_S.

- The presence of multiple modes contributing to a peak is a drawback that can be overcome in many situations. In the case of dyes, it is not unusual for several Raman active modes, which are closely spaced in energy and have different cross-sections, to contribute to the observed peaks. This will naturally result in distortions of the line shape and problems with any estimate of the lifetime based on the width of the peak. This can be overcome by the use of well characterized vibrations which are relatively isolated from the others and even (if possible) complementing the information by density functional theory (DFT) calculations of the Raman spectra[24,25] to support the selection of those modes that are the best candidates for a reliable estimation of τ.

- If the broadening is homogeneous,[26] the only remaining contributions to the line width are the diagonal and off-diagonal relaxation times. Molecular vibrations have typically very strong anharmonic couplings with other vibrations in the molecule and contributions to inhomogeneous broadenings are mostly negligible. Even in SERS experiments where the single molecule limit is approached[27] (which would be more sensitive to inhomogeneous broadening) the full width at half-maximum (fwhm), Γ, of the peaks does not change by more than $1-1.5$ cm^{-1} in peaks with a typical Γ of $\sim 15-20$ cm^{-1}. The validity of this assumption (whether inhomogeneous broadening is important or not) has to be assessed obviously in each specific situation.

- The separation between diagonal and off-diagonal relaxation times cannot be achieved by a simple SERS spectrum. It is always possible to invoke a different type of spectroscopy (time resolved),[23] but this may not be feasible in most situations. One simple possibility (as done in ref 20) is to estimate the population relaxation by using the fwhm (Γ) of the peaks via $\tau \sim \hbar/\Gamma$; i.e., essentially ignoring the contribution of the dephasing (off-diagonal) relaxation to the width. This will produce an underestimation of τ and an overestimation of σ_S. In addition, this typically produces cross-sections for different peaks which are not entirely consistent with the relative (integrated) intensities among peaks; thus showing an intrinsic inconsistency in the estimation of the τs (which can be of the order of a factor of

2−10 for the examples we examined). It is generally difficult to make a simple estimation that will be valid for all modes. It is quite clear that for the cross-sections to be meaningful (and if they are not affected by different amounts of nonradiative processes) the relative cross-sections among peaks must be in accordance with the relative integrated intensities observed in a normal SERS spectrum.

•Population relaxation is caused mainly by the anharmonic coupling to the "thermal bath". This bath includes all other modes in the molecule as well as those in the solvent or substrate. Generally speaking, higher energy modes have shorter lifetimes due to a greater number of possible decay pathways. Intramolecular anharmonic decays are energy conserving, meaning that high energy modes have more possibilities for a decay than low energy ones.

•It is important to realize that, in principle, *if we find a single peak in the spectrum where the population relaxation can be gained directly from the fwhm via* $\tau \sim \hbar/\Gamma$, *then all of the cross-sections of the other modes follow immediately through the relative integrated intensities of the peaks*. When lacking a time-resolved experiment to isolate the contributions properly, *the problem comes down to a judicious choice of a mode where the width is dominated by population relaxation*. A compromise then is to extract the values of the cross-sections by means of the width of one of the highest frequency (isolated) Raman active modes. A rule of thumb is that the lower the temperature and the higher the energy of the mode the more the line width will be dominated by population relaxation. We can then use one mode to estimate its σ_S, and all the others follow automatically from this assumption. The cross sections are now consistent by construction and the method provides, in fact, the means to estimate the relative lifetimes of the modes. We call this procedure (i.e., estimating the τ of one Raman active mode and making the other cross-sections consistent with this value through the relative integrated intensities), the *corrected lifetime method* (CLM).

•The selection of a suitable reference peak dominated by population relaxation is the key step. Once this peak is chosen (and its lifetime calculated via $\tau \sim \hbar/\Gamma$), we use it to determine the cross-sections of other peaks through their relative Stokes intensities. Let us call the cross-section and lifetime of the reference peak $\sigma_S^{Ref.}$, and $\tau^{Ref.}$, respectively. The integrated Stokes intensity of this peak will be called $I_S^{Ref.}$. The cross-sections for the *i*th peak can be readily obtained from the following:

$$\sigma^i_S = \frac{I^i_S}{I_S^{Ref.}}\sigma_S^{Ref.} \tag{10}$$

Once the σ^is have been determined, we can calculate the corresponding population relaxations for the *i*th mode (τ^i) by using the experimental value of ρ in the plateau region below T_{cr} (given by eq 9) which is $A\tau^i\sigma_S{}^iI_L/\hbar\omega_L$. For self-consistency, we need to check that none of the so-obtained τ^i's are smaller than the value of $\hbar/\Gamma^i$ obtained from their widths Γ^i. The lifetimes, τ^i, can only be *larger* than (or equal to) $\hbar/\Gamma^i$ to account for the existence of the dephasing relaxation time. If this is not the case, the choice of the reference peak was not the most appropriate. The strategy is then to go in decreasing order of energy among the Raman active modes in the spectrum until this condition is fulfilled for one of them. This is the best guess for a consistent determination of cross-sections based on a mode with a likely large contribution from population relaxation and that respects the minimum broadening observed experimentally in the other peaks. The reference mode is then specified in each case for each data analysis.

•If we are comparing different substrates with the same analyte, we could also directly compare the values of $\tau\sigma_S$ without any further assumption. If there is no reason to believe that the relaxation lifetime is different between the two substrates, *the ratio of* $\tau\sigma_S$ *for two different substrates provides a direct comparison of SERS cross sections*.

C. The Asymmetry Factor. Problems with measuring the asymmetry factor "*A*" can be as important as those to obtain a reliable lifetime. Heating in the thermally dominated regime can be a *major* problem. As demonstrated in Section II B, heating can be in part a source for a larger than normal *A*, if it is not properly identified. As we shall show later, heating can be identified in the pumping data by the inclusion of an additional parameter in the fit. This compensates partially for the problem and makes the estimation of *A* more reliable, even in the presence of a moderate amount of laser heating.

Ideally, the best estimation of *A* can come from measurements at RT with long integration times and very low powers. For the same laser excitation, the obtained *A*s should be more or less the same for a given analyte in the presence of the same metal (they are mainly related to the local interaction of the dye with the metal.[22]).

The product $A\tau\sigma_S$ is measured with high accuracy in the pumping dominated "plateau" at low temperatures. Accordingly, the best use of the technique is to use one well-characterized analyte (without photobleaching if possible) as a means to compare the relative SERS cross-sections of the dye on different substrates of the same metal, by simple comparison of the plateaus. The product $A\tau\sigma_S$ is perhaps the best "objective" comparison between the cross-sections of two substrates without any assumption. However, it is also important to note that the cross-sections we are comparing are not the average cross-sections, but rather a biased average toward the highest cross-sections in the sample, as explained in the next subsection.

D. Which Cross-Section do we Really Measure?. There are additional complications with the estimation of the cross-section. It is generally accepted that SERS signals are dominated by the presence of "hot-spots" or places with high local enhancements. The formulas presented above made implicitly the assumption that the cross-section is the same for all *N* molecules in the sample. The question we want to address now is, do we obtain an estimate of the average cross-section with this method? We shall show in what follows that what we actually obtain from the experiment is an estimate which is heavily biased toward the sites with the highest enhancements; i.e., the method provides an estimate of the enhancements in hot-spots. This is, of course, an advantage and a disadvantage at the same time. We show this explicitly in this section.

We consider a number of molecules (*i* from 1 to *N*) in the sample. Each molecule can have a different anti-Stokes, ($\sigma_{aS}{}^i$) and Stokes ($\sigma_S{}^i$) SERS cross-sections (according to the asymmetry factor $A^i = \sigma_{aS}{}^i/\sigma_S{}^i$ for that molecule). We assume for simplicity that the incident power I_L is the same for all. The rate equation for the average phonon population n^i of a vibrational mode of *one molecule*, *i*, and its stationary state solution are given by expressions similar to eqs 1 and 2: Following the other formulas in the previous sections, the Stokes signal for this molecule is simply $I_S{}^i = \sigma_S{}^iI_L$, while the anti-Stokes signal is given by $I_{aS}{}^i = n^i\sigma_{aS}{}^iI_L$. The anti-Stokes/Stokes ratio *for this molecule*, ρ^i, is given by an expression similar to eq 5. If all the molecules experienced the same enhancements, then the total Stokes and anti-Stokes intensities would be $I_S =$

NI_S^i and $I_{aS} = NI_{aS}^i$, and the ratio would be $\rho = \rho_i$. However, if the molecules have different cross-sections (SERS enhancements), which is a much more realistic assumption, we then have

$$I_S = \sum_{i=1}^{N} \sigma_S^i I_L \tag{11}$$

$$= N\langle\sigma_S\rangle I_L, \tag{12}$$

and

$$I_{aS} = \sum_{i=1}^{N} \sigma_{aS}^i I_L \left(\frac{\tau \sigma_S^i I_L}{\hbar\omega_L} + e^{-\hbar\omega_\nu/k_BT} \right) = N\langle\sigma_{aS}\sigma_S\rangle I_L \frac{\tau I_L}{\hbar\omega_L} + N\langle\sigma_{aS}\rangle I_L e^{-\hbar\omega_\nu/k_BT} \tag{13}$$

All the averages here $\langle ... \rangle$ are the usual statistical ensemble averages. The aS/S-ratio is then

$$\rho = I_{aS}/I_S = \frac{\langle\sigma_{aS}\rangle}{\langle\sigma_S\rangle}\left[\frac{\langle\sigma_{aS}\sigma_S\rangle}{\langle\sigma_{aS}\rangle}\tau\frac{I_L}{\hbar\omega_L} + e^{-\hbar\omega_\nu/k_BT}\right] \tag{14}$$

Comparing this expression with that obtained previously in eq 5, what we called A is now replaced by

$$A^E = \frac{\langle\sigma_{aS}\rangle}{\langle\sigma_S\rangle}. \tag{15}$$

Note that this is not exactly the average of the A^i's, i.e., $\langle A\rangle$. Moreover, what we measure (instead of $\tau\sigma_S$) is now

$$\tau\sigma_S^E = \tau\frac{\langle\sigma_{aS}\sigma_S\rangle}{\langle\sigma_{aS}\rangle} \tag{16}$$

To understand the meaning of σ_S^E (E for ensemble), we need to understand the sources of nonuniformity. The main variation is in the cross-sections, because of the large differences in SERS enhancements at different locations on the SERS substrate. We typically have values which are, for example, 10^3-10^6 larger at hot-spots than in other places. However, for a given molecule, the ratio $A^i = \sigma_{aS}^i/\sigma_S^i$ should not vary as much (at least not by more than 1 order of magnitude). In fact, this ratio can, in a first approximation, be taken as a constant, which is an intrinsic property of the adsorbed molecule/metal complex.[22] Assuming that $A^i = A$ is the same for all molecules, we simply get that $A^E = A$, i.e., the A we measure is the correct one. Moreover, using $\sigma_{aS}^i = A\sigma_S^i$, we can express σ_S^E as a function of σ_S^i only as

$$\sigma_S^E = \frac{\langle\sigma_S^2\rangle}{\langle\sigma_S\rangle} \tag{17}$$

If the distribution of σ_S's were fairly uniform (for example a Gaussian around an average value with a small standard deviation), then σ_S^E would be a good estimate of the average of the distribution (slightly overestimated). But this is far from reality in SERS conditions. A more realistic situation is to have a small number of molecules at a hot-spot (HS), and a large number of molecules at non-HS positions. For the sake of argument, let us demonstrate the effect on this average by considering 10^3 molecules with one molecule at a HS and 999 molecules at places with much lower enhancements. The expression given above would give the following:

$$\sigma_S^E = \frac{1/1000(1(\sigma_S^{HS})^2 + 999(\sigma_S^{NHS})^2)}{1/1000(1(\sigma_S^{HS}) + 999(\sigma_S^{NHS}))} \tag{18}$$

If there is a difference of a few orders of magnitude between the cross-sections σ_S^{HS} and σ_S^{NHS}, the numerator is then easily dominated by the one molecule at the HS (due to the square). For the denominator, it is not as clear-cut, it all depends on how much stronger the HS is and how many molecules are at non-HS positions. But overall, the denominator is likely to be dominated by σ_S^{HS}, possibly slightly larger if the second contribution is not negligible. This shows that $\sigma_S^E \approx \sigma_S^{HS}$, or perhaps slightly smaller. A more quantitative argument is only possible if we had a more realistic distribution of SERS enhancements for a given substrate, but the qualitative conclusion is that *pumping experiments provide a good lower estimate (because of the influence of the rest of the distribution) of the cross-section of the few molecules experiencing the highest enhancements*.

E. Photobleaching. The last aspect we want to briefly touch upon in this analysis of cross-section estimations via vibrational pumping is photobleaching. The exact mechanisms of photobleaching under SERS conditions are still poorly understood and would deserve a full study in itself. Photobleaching is particularly important in the method we are describing here because molecules sited at HS's (i.e., those exposed to the largest enhancements) are likely to be affected to a greater degree. At high power densities, for example, the population of molecules at HS's may be bleached at a faster rate than the average and this will change the measured cross-section. Studying ρ under photobleaching conditions could, in fact, tell us something about this distribution. There is robust experimental evidence that photobleaching can complicate the analysis, produce experimental artifacts, and to a large extent, even decide the answer we obtain from a specific experiment. This is added to several experimental complications in aS/S, ratios which include the fact that sometimes (depending on the dispersion of the spectrometer) the anti-Stokes and Stokes sides cannot be measured simultaneously. This implies a delay between the two measurements, and therefore, a difference in exposure times to the laser. By choosing a certain power level we are, in a way, selecting the population of HS's that we are going to measure. We shall come back to this problem in the discussion of the results. A rule of thumb is that larger laser spots with low power densities (but sufficient to produce detectable pumping), short integration times, and nonresonant (with the dye) laser excitation, are in general preferable for a more reliable estimate of SERS cross sections. All possible measures should be taken (including the type of scanning used) to address and minimize the undesirable effects of photobleaching.

IV. Experimental Section

We turn now to an experimental demonstration of the principles underlined above. SERS measurements have been performed on substrates formed by dried Ag colloids on silicon. The colloids were prepared using the standard Lee and Meisel technique.[28] SERS active samples were prepared by mixing the colloids with a 20 mM KCl solution in equal amounts. The analytes were then added to give a concentration of 10^{-6} M in each case. A small amount of this solution was then dried on

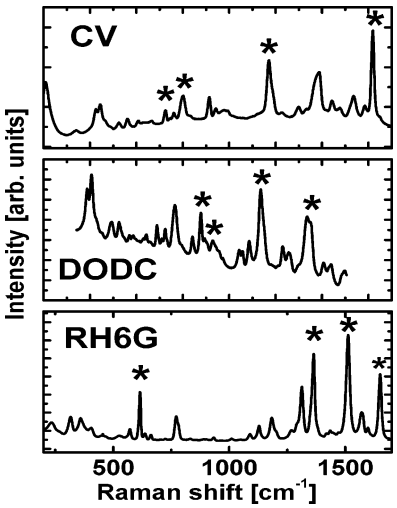

Figure 2. SERS spectra of the three analytes used in this paper taken with a 633 nm laser: crystal violet (CV, top), 3,3′-diethyloxadicarbocyanine (DODC, center), and rhodamine 6G (RH6G, bottom). The temperature dependence of the aS/S-ratios of the peaks labeled with "*" are explicitly shown in Figure 4. Tables 1 and 2 include estimations of cross-sections for additional peaks not labeled here.

to a silicon substrate. The investigated analytes are rhodamine 6G (RH6G), crystal violet (CV), and 3,3′-diethyloxadicarbocyanine (DODC). Figure 2 shows the basic SERS spectra of the analytes at the same excitation wavelength (633 nm). We shall show the explicit temperature dependencies of the aS/S-ratios for only a few modes (labeled in Figure 2) while the tables show additional data for other modes. Samples were mounted in a closed-cycle He-cryostat (CTI-Cryogenics) with temperature control in the range 10−300 K. Raman measurements were performed using several laser lines of a Kr^+ and Ar^+-ion lasers which were focused to a 20 μm diameter spot. The signal was collected using a high-numerical aperture photographic zoom lens (Canon, ×10 magnification) onto the entrance slit of a high-dispersion double-additive U1000 Jobin-Yvon spectrometer coupled to a liquid N_2-cooled CCD detector. Peaks were analyzed using standard Voigt functions with subtracted backgrounds. The variation in the aS/S-ratio with T for each mode was then fitted to eq 5. For this purpose, it is convenient to modify the expression to the following:

$$\ln(\rho) = a + \ln[b + e^{-\hbar\omega_\nu/k_B T}] \qquad (19)$$

where $a = \ln(A)$, and $b = \tau\sigma_S I_L/\hbar\omega_L$ which are the (dimensionless) fitted parameters. The τs of the peaks (necessary to obtain the cross-sections) are estimated in two different ways following the prescriptions in Section III B.

As discussed earlier, it is of critical importance that the sample remains stable over the entire length of the experiment. Power densities were kept to a minimum compatible with the observation of pumping and exposure to the beam was minimized as much as possible between changes of T. We used 50 mW spread over the 20 μm diameter spot. This implies a power density for all measurements of the order of 1.3×10^8 W/m^2, which is an order of magnitude smaller than the typical power densities used in Raman microscopes. As the rate of photobleaching may change with T[29] a suitable power density to ensure reasonable stability must be decided at RT, where the effect is greatest. The relatively large spot and low power densities have the triple advantage of (i) reducing photobleaching to a negligible level, (ii) reducing any indirect laser heating effects, and (iii) improving the averaging over cluster geometries. Still, even under low

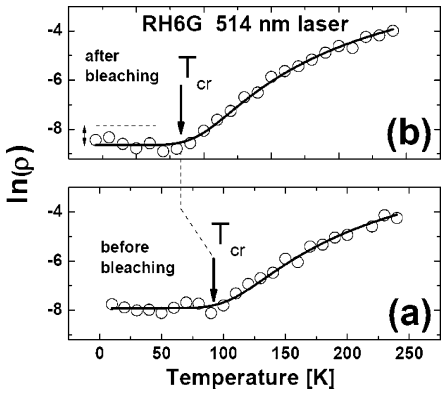

Figure 3. Effect of photobleaching on the temperature dependence of the aS/S-ratio for the 610 cm^{-1} mode of RH6G at 514 nm excitation. The measurement in (a) is performed at low power density (25 mW on a 20 μm spot in diameter). The sample is then exposed to 400 mW for 3 min on the same spot and the measurement is repeated afterward with the same original low power density. The decrease in the plateau of ln(ρ) to smaller values (and the associated shift of T_{cr} to lower temperatures) in (b) is consistent with a bleaching of the molecules on the HS's with the highest enhancement in the first measurement. The dashed line in (b) is the value at which ln(ρ) tails in (a). By choosing a certain power level, we are selecting the population of HS's that will survive through the experiment. We are therefore measuring a convoluted property of the substrate and the photostability of the probe.

power density excitation, the choice of laser line can have an important effect on the measurement. An explicit example is shown in Figure 3 for the 610 cm^{-1} mode of RH6G under 514 nm excitation. As explained in the caption, this observation is compatible with a bleaching of the HS's with largest cross-sections. Laser lines that are strongly resonant with the probe molecule[22] should be avoided when possible so that the photostability of the analyte and the accumulated exposure to the laser do not become an issue in the interpretation and analysis of the data. If this situation is not achievable the effect of heating coexisting with pumping might have to be taken into account (as we shall show in the next section). We only concentrate hereafter on results obtained with the 647 and 676 nm lines of a Kr^+-laser. These two lines are close enough to the visible (to profit fully from SERS enhancements) but, by the same token, they do not produce excessive photobleaching for the dyes under consideration here.

V. Results and Discussion

Having all the theoretical tools from the previous sections, we can now easily scan through several experimental results that demonstrate the method in practice. Figure 4 shows the aS/S-ratios (ln(ρ)) vs T, as measured using the 676 nm line, for four modes of each of the investigated analytes. The solid lines represent the best fit to the experimental values using eq 19. A series of small imperfections can be seen in the data for some modes, but overall the behavior is very well represented by eq 19, with RH6G being the best example. The arrows indicate the crossover points (T_{cr}) between the thermally dominated and pumping-dominated regimes for all the investigated modes. T_{cr} occurs at higher Ts for higher energy modes, as expected. The fact that pumping is observed for each of the modes indicates that the effect is fairly general and should be observable for a large number of analytes for as long as σ_S is high enough to make pumping observable at moderate power densities.[30]

It is interesting to note that of the three dyes shown in Figure 4 at 676 nm laser excitation, DODC is the one that does not quite follow eq 19 as well as the other dyes, unless an additional

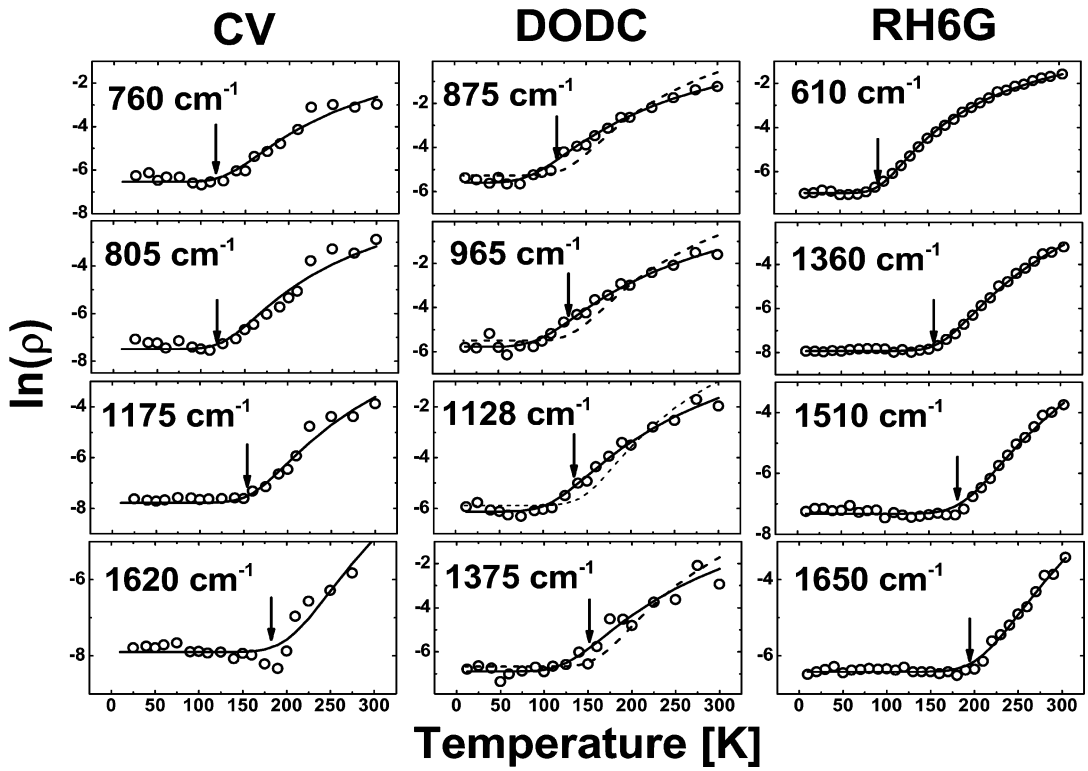

Figure 4. Anti-Stokes/Stokes ratios ($\ln(\rho)$) as a function of temperature for four modes of each of the analytes investigated here (all taken using 676 nm excitation). The arrows indicate the crossover points between the thermally dominated and pumping-dominated regimes. Note that the cross over occurs at different temperatures for different modes, being at higher T's for larger vibrational energies. The solid lines represent the best fit to the experimental data using eq 19. DODC needs the inclusion of a heating parameter ($\Delta T = 50$ K) to achieve a satisfactory fit (unlike RH6G and CV). The figures for DODC show fits with both eq 19 (no heating: dashed line) and eq 20 (heating: solid line). Table 2 presents an analysis of these data using different assumptions for the lifetimes.

TABLE 1: Values of $b = \tau\sigma_S I_L/\hbar\omega_L$, τ, Relative Integrated Intensities, and Cross-sections of the Stokes Modes[a]

		widths					corrected				
mode (cm^{-1})	b ($\times10^{-5}$)	τ(ps)	rel. I_S rel. σ_S	σ_S (cm^2) (	$\times10^{-15}$)	σ_{aS} (cm^2) ($\times10^{-15}$)	τ (ps)	rel. I_S	rel. σ_S	σ_S (cm^2) ($\times10^{-15}$)	σ_{aS} (cm^2) ($\times10^{-15}$)
610	25.6	0.8	0.9	11.5	6.0	22.0	10.4	0.9	0.9	0.5	1.7
780	6.9	0.2	1.1	11.2	5.9	28.2	2.3	1.1	1.1	0.6	2.7
1360	1.3	0.5	1.0	1.0	0.5	14.3	0.5	1.0	1.0	0.5	14.3
1510	2.1	0.3	1.7	2.6	1.4	42.1	0.4	1.7	1.7	0.9	28.3
1650	2.1	0.3	0.6	2.4	1.2	94.8	1.3	0.6	0.6	0.3	23.5

[a] The values of σ_S and σ_{aS} are shown for two analysis schemes: (i) τs obtained from the fwhm of the peaks (ignoring dephasing contributions) and (ii) corrected τs to account for the relative integrated intensities (CLM method with reference mode 1360 cm^{-1}). Note that the τs from CLM with this reference peak are *larger* than the broadening limited τs, as required. All data are for RH6G using the 676 nm laser line as excitation. The "rel. I_S" column is obtained directly from the relative integrated intensities of the peaks in the SERS spectrum. We do not quote error bars because the overriding cause of error in these numbers is *systematic* (rather than statistical) and comes from the estimation of τ itself.

degree of freedom is allowed for in the form of laser heating (ΔT). This implies using

$$\ln(\rho) = a + \ln[b + e^{-\hbar\omega_\nu/k_B(T+\Delta T)}] \qquad (20)$$

Instead of eq 19. Figure 4 shows fits with and without the extra parameter ΔT for the case of DODC for the 676 nm laser. The existence of direct laser heating (coexisting with pumping) in DODC is consistent with direct photon absorption for this dye implying it is closer to the direct resonance condition with the laser at 676 nm. The other two dyes achieve a high quality fit to eq 19 without evidence of heating. The pragmatic approach we have used here is to start with eq 19 and introduce an additional heating parameter in the fit as in eq 20 only if the curvature of the S-shaped experimental pumping data of $\ln(\rho)$ vs T require it. This is an important judgment to be made, for a fit with or without ΔT will achieve different values for the asymmetry parameter A and, therefore, affect the estimation of the cross section through the plateau in ρ at low temperatures (which is proportional to A).

To transform these data into estimates of the cross sections we need to address the different methods of estimating τ. Table 1 shows the experimental results for RH6G taken with the 676 nm line. For the sake of comparison, we display the cross-section by using two different estimations of the τs. This gives a better idea of how reliable these numbers are and how differences among them should be interpreted. Table 1 shows both (i) the extraction of τ directly from the widths via $\tau\sim\hbar/\Gamma$ (this normally renders cross-sections which are not fully consistent with the relative integrated intensities of the peaks) and (ii) the extraction of τ from the CLM method described in Section III B using a reference mode (1360 cm^{-1} in this case). A column with relative intensities and cross-sections among modes is also provided for completeness. The anti-Stokes cross-sections are obtained through the Stokes ones via the fitted value of the asymmetry

TABLE 2: Cross-Section for the Stokes and Anti-Stokes Raman Modes of CV, RH6G and DODC Extracted from $b = \tau\sigma_S I_L/\hbar\omega_L$ Obtained through Fitting the Experimental Data to Eq 19 (or Eq 20 for DODC) for Both the 647 and 676 nm Lasers[a]

	647 nm			676 nm		
mode (cm^{-1})	σ_S (cm^2) ($\times10^{-15}$)	σ_{aS} (cm^2) ($\times10^{-15}$)	b ($\times10^{-5}$)	σ_S (cm^2) ($\times10^{-15}$)	σ_{aS} (cm^2)	b ($\times10^{-5}$)
RH6G						
610	0.9	4.7	48.5	0.5	1.7	25.6
780	2.2	12.0	27.6	0.6	2.7	6.9
1360	1.7	14.3	4.0	0.5	14.3	1.3
1510	2.6	36.8	5.7	0.9	28.3	2.1
1650	3.1	57.8	21.4	0.3	23.5	2.1
DODC						
875	2.1	15.3	20.4	1.8	18.8	36.0
925	2.0	19.5	16.3	1.9	19.4	42.7
965	2.0	18.9	13.9	2.2	29.8	22.9
1128	2.9	27.2	9.8	3.4	67.6	11.1
1375	0.5	11.7	2.8	2.0	53.7	3.8
CV						
760	1.0	1.3	93.5	0.1	0.25	57.4
805	8.0	10.6	74.7	1.7	3.2	31.7
910	2.8	4.8	124.1	0.5	1.9	7.1
1175	14.2	22.4	18.0	2.1	15.2	6.5
1292	2.7	4.5	8.4	0.8	2.3	4.1
1620	4.6	10.5	10.0	1.0	16.2	2.2

[a] The reference mode for the CLM is always the peak with the highest Raman shift in the spectra, except for RH6G for which we use the 1360 cm^{-1} mode (to make the τs compatible with the broadening of the peaks). For RH6G at 647 nm we used the same τs obtained for 676 nm due to the much higher quality of the data in this latter case. The τs of the modes are expected to be fairly insensitive to laser excitation; i.e., if the lifetimes for one laser are very reliable (due to the quality of the data) they can be, in principle, transferred to the analysis of other laser excitations. See the text for further details.

parameter A from eq 19. These results prove the point that the estimation of the lifetime is a crucial step in this method to transform the experimental values into an estimation of the cross-sections themselves. The values should be interpreted within this assumption, and their validity should be assessed on a case-by-case basis. The preferred (more consistent) method is of course the one that ensures the relative cross sections agree with the relative intensities of peaks (CLM in Section III B).

Finally, we can discuss the effect of estimating the cross-sections for two different excitation wavelengths. The experiment is somewhat restricted in the choice of excitations (to be compatible with photostability) but still provides a hint of resonance contributions to the cross-sections with some limitations. Table 2 shows the cross-sections obtained for RH6G, DODC, and CV for 647 and 676 nm excitations for different modes. All the cross-sections were obtained by the CLM analysis. The highest energy mode was found to be the most acceptable reference peak for CLM (as expected) for both DODC and CV, but not for RH6G. In this case the 1360 cm^{-1} mode was found to be the best choice. The RH6G data obtained with the 647 nm laser was of considerably lower quality than that obtained using the 676 nm laser. This resulted in an unphysical estimation of τs. As a result, the lifetimes calculated at 676 nm with the CLM method were used for the data at 647 nm. It is worth noting that in this latter method we only need (in principle) one temperature dependent aS/S-ratio for the reference mode (judged to be dominated by population relaxation). This together with the plain SERS spectrum of the dye is enough (in principle) to estimate all the cross-sections of the modes via the relative integrated intensities. The results will be consistent (by construction) but not necessarily accurate (depending on the choice of reference mode). The main conclusions of these experiments can be summarized as follows: (i) RH6G shows larger cross-sections at 647 than at 676 nm (by on average a factor of $\sim$3). This is consistent with a resonant increase known to exist in RH6G toward the yellow part of the spectrum.[22] (ii) CV also shows larger cross-sections at 647 than at 676 nm (by on average a factor of 6) but overall similar enhancements to RH6G. (iii) The cross-sections calculated for DODC is similar at both excitation frequencies suggesting a very broad resonance profile in this range. (iv) Broadly speaking, the CLM method predicts vibrational lifetimes that lie within the range $\sim$0.1$-$10 ps, which compare reasonably well with typical vibrational lifetimes obtained from time-resolved spectroscopy.[26]

The values in Tables 1 and 2 deserve a special comment regarding their interpretation. For a start, the main source of potential error (as pointed out in the caption of Table 1) is systematic rather than statistical, and comes from the different methods used in the estimation of τ. Error bars for these systematic errors are not easy to obtain from the data, for they depend on the relative contribution to the fwhm of population relaxation and dephasing, which is unknown and changes from mode to mode. The number of significant figures has been decided by the range of values for a given group of modes and laser excitation. The order of magnitude of these values deserves a special comment too. The method provides a good estimate of the highest cross sections available in a specific substrate (compatible with experimental parameters such as photobleaching) and, accordingly, the estimations should be compared not to *average* cross sections found commonly in many applications but rather to cross sections compatible with single molecule SERS. The most consistent set of values are obtained using the CLM method (which is the preferred option) and are all of the order of $\approx10^{-15}$ cm^2. In a few cases, cross-sections of the order of $\approx10^{-14} - 10^{-13}$ cm^2 are obtained (with the addition of resonance effects, as in the case of DODC). All these values are within what is expected from estimations of cross sections compatible with single molecule observations in SERS and with enhancement factors of the order of $10^{10} - 10^{12}$. In addition, if the absolute magnitude of the cross sections is not an issue, the method makes it possible to compare $\tau\sigma_S$ (or $A\tau\sigma_S$) for the same modes in different substrates providing an unbiased relative comparison of performances.

VI. Conclusions

We have presented an in-depth discussion of the state-of-the-art of SERS cross-section estimation via vibrational pumping and have given several experimental examples of it. Despite the approximations needed and the intrinsic problems of the technique, it is still an excellent tool (and in many cases possibly the only tool) to extract an estimation of the SERS cross-sections in situations where the number of molecules and hot-spots present in the sample are not known or are difficult to estimate. The *self-normalizing* nature of the method (with respect to the number of molecules involved) is certainly a major advantage. In addition, we feel that these latter experimental and theoretical developments have moved forward to establish vibrational pumping as a real phenomenon in SERS after almost a decade of controversy about its very existence.

Taking into account that this method gives a good estimate of the highest cross-sections in these substrates, the experimental values for the cross-sections are in agreement with the expectations coming from single-molecule detection SERS and with the expected electromagnetic enhancements obtained in simula-

tions (taking into account that the SERS enhancement is proportional to the fourth power of the electric field[31]).

One outstanding issue that surely deserves further investigation is the effect of photobleaching under SERS conditions (in particular in HS). As we showed in Section III D, the fact that this technique produces an estimate of the cross-sections which is heavily biased toward HS's provides a unique opportunity to explore their characteristics. This is particularly true in the comparison among different substrates (in which the photostability of the analyte plays a special role). A forthcoming study on the topic is in preparation.

Acknowledgment. P.G.E. and L.F.C. acknowledge support by EPSRC (UK) under grant GR/T06124. R.C.M. acknowledges partial support from the National Physical Laboratory (UK) and the hospitality of the MacDiarmid Institute at Victoria University (New Zealand) where the measurements have been performed. Special thanks are given to Dominik Hangleiter (Wellington College, NZ) for taking the data in Figure 3.

References and Notes

(1) Moskovits, M. *Rev. Mod. Phys.* **1985**, *57*, 783.

(2) Perney, N. M. B.; Baumberg, J. J.; Zoorob, M. E.; Charlton, M. D. B.; Mahnkopf, S.; Netti, C. M. *Opt. Express* **2006**, *14*, 847.

(3) Green, M.; Liu, F. M. *J. Phys. Chem. B* **2003**, *107*, 13015.

(4) Drachev, V. P.; Thoreson, M. D.; Nashine, V.; Khaliullin, E. N.; Ben-Amotz, D.; Davisson, V. J.; Shalaev, V. M. *J. Raman Spectrosc.* **2005**, *36*, 648.

(5) Jackson, J. B.; Westcott, S. L.; Hirsch, L. R.; West, J. L.; Halas, N. J. *Appl. Phys. Lett.* **2003**, *82*, 257.

(6) Lyandres, O.; Shah, N. C.; Yonzon, C. R.; Walsh, J. T.; Glucksberg, M. R.; Van Duyne, R. P. *Anal. Chem.* **2005**, *77*, 6134.

(7) Larsson, M.; Lindgren, J. *J. Raman Spectrosc.* **2005**, *36*, 394.

(8) Rasmussen, A.; Deckert, V. *J. Raman Spectrosc.* **2006**, *37*, 311.

(9) Cinta-Pinzaru, S.; Peica, N.; Kustner, B.; Schlucker, S.; Schmitt, M.; T. Frosch, Faber, J. H.; Bringmann, G.; Popp, J. *J. Raman Spectrosc.* **2006**, *37*, 326.

(10) Binoy, J.; Joe, I. H.; Jayakumar, V. S.; Nielsen, O. F.; Aubard, J. *Laser Phys. Lett.* **2005**, *2*, 544.

(11) Szeghalmi, A. V.; Leopold, L.; Pinzaru, S.; Chis, V.; Silaghi-Dumitrescu, I.; Schmitt, M.; Popp, J.; Kiefer, W. *Biopolymers* **2005**, *78*, 298.

(12) Sylvia, J. M.; Janni, J. A.; Klein, J. D.; Spencer, K. M. *Anal. Chem.* **2000**, *72*, 5834.

(13) Kneipp, K.; Wang, Y.; Kneipp, H.; Itzkan, I.; Dasari, R. R.; Feld, M. S. *Phys. Rev. Lett.* **1996**, *76*, 2444.

(14) Brolo, A. G.; Sanderson, A. C.; Smith, A. P. *Phys. Rev. B* **2004**, *69*, 45424.

(15) Haslett, T. L.; Tay, L.; Moskovits, M. *J. Chem. Phys.* **2000**, *113*, 1641.

(16) Le Ru, E. C.; Etchegoin, P. G. *Faraday Discuss.* **2006**, *132*, 63.

(17) Teredesai, P. V.; Sood, A. K.; Govindaraj, A.; Rao, C. N. R. *Appl. Surf. Sci.* **2001**, *182*, 196.

(18) Maher, R. C.; Cohen, L. F.; Le Ru, E. C.; Etchegoin, P. G. *Faraday Discuss.* **2006**, *132*, 77.

(19) Maher, R. C.; Cohen, L. F.; Gallop, J. C.; Le Ru, E. C.; Etchegoin, P. G. *J. Phys. Chem. B* **2006**, *110*, 6797.

(20) Maher, R. C.; Etchegoin, P. G.; Le Ru, E. C.; Cohen, L. F. *J. Phys. Chem. B* **2006**, *110*, 11757.

(21) Kneipp, K.; Kneipp, H.; Kartha, V. B.; Manoharan, R.; Deinum, G.; Itzkan, I.; Dasari, R. R.; Feld, M. S. *Phys. Rev. E* **1998**, *57*, R6281.

(22) Maher, R. C.; Hou, J.; Cohen, L. F.; Liu, F. M.; Green, N.; Brown, R. J. C.; Milton, M. J. T.; Le Ru, E. C.; Hadfield, J. M.; Harvery, J. E.; Etchegoin, P. G. *J. Chem. Phys.* **2005**, *123*, 84702.

(23) Laubereau, A.; Kaiser, W. *Rev. Mod. Phys.* **1978**, *50*, 607.

(24) Watanabe, H.; Hayazawa, N.; Inouye, Y.; Kawata, S. *J. Phys. Chem. B* **2005**, *109*, 5012.

(25) Naumov, S.; Kapoor, S.; Thomas, S.; Venkateswaran, S.; Mukherjee, T. *J. Mol. Struct.* (THEOCHEM) **685**, 127 (2204).

(26) Demtröder, W. *Laser Spectrosopy;* Springer-Verlag: Berlin, 2003.

(27) Le Ru, E. C.; Meyer, M.; Etchegoin, P. G. *J. Phys. Chem. B* **2006**, *110*, 1944.

(28) Lee, P. C.; Meisel, D.; *J. Phys. Chem.* **1982**, *86*, 3391.

(29) Pieczonka, N. P. W.; Aroca, R. F. *Chem. Phys. Chem.* **2005**, *6*, 2473.

(30) Measurements on adenine with these lasers showed no signs of optical pumping, suggesting that the cross-section is small relative to the analytes used here.

(31) Le Ru, E. C.; Etchegoin, P. G. *Chem. Phys. Lett.* **2006**, *423*, 63.

(32) Le Ru, E. C.; Galloway, C.; Etchegoin, P. G. *Phys. Chem. Chem. Phys.* **2006**, *8*, 3083.